Structure of a G48H mutant of HIV-1 protease explains how glycine-48 replacements produce mutants resistant to inhibitor drugs

Lin Hong[a], Xue-Jun Zhang[a], Steve Foundling[a], Jean Ann Hartsuck[a,b], Jordan Tang[a,b,*]

[a] *Protein Studies and Crystallography Programs, Oklahoma Medical Research Foundation, Oklahoma City, OK 73104, USA*
[b] *Department of Biochemistry and Molecular Biology, University of Oklahoma Health Sciences Center, Oklahoma City, OK, USA*

Received 13 October 1997; revised version received 14 November 1997

Abstract The crystal structure of human immunodeficiency virus type 1 (HIV-1) protease mutant G48H with peptidic inhibitor U-89360E is described. Comparison with wild-type protease-inhibitor complex shows that mutation of flap residue 48 to histidine allows stabilizing van der Waals contacts between the side chains of His^{48} and Phe^{53} as well as between His^{48} and the P_2' and P_3' inhibitor subsites. The flap region is less mobile than in the wild-type enzyme. A model of saquinavir-resistant mutant protease G48V in complex with saquinavir predicts interactions similar to those found in the G48H crystal. Energetic calculations confirm the similarity of the His^{48} and Val^{48} interactions.

Key words: HIV protease; Mutation; Saquinavir; Drug resistance

1. Introduction

Therapeutic efforts against the human immunodeficiency virus type 1 (HIV-1) are handicapped by the development of drug resistance. The facile mutation and rapid replication of the virus both contribute to rapid selection of resistant mutants in the presence of inhibitor drugs [1]. Specific mutation positions in HIV-1 protease are now known to confer in vivo HIV-1 resistance to several inhibitor drugs [2–4], including three marketed HIV-1 protease inhibitor drugs: saquinavir (Ro 31-8959) [5], indinavir (L-735,524) [6], and ritonavir (ABT-538) [7]. The mutation of Gly^{48} to valine in HIV-1 protease contributes to viral resistance against sasquinavir [4]. The kinetics of Gly^{48} mutants, compared to those of the wild-type protease, are consistent with the resistant properties [8–10]. However, the structural basis for these mutation evoked property changes has not been determined. The structural changes related to Gly^{48} mutation are of particular interest because the crystallographic studies of inhibitor-resistant HIV-1 protease mutants have so far dealt with mutations in substrate binding pockets [11–14]. No structural information is available for resistant mutations in the mobile protease flap (residues 45 to 55), even though several flap residues are mutated in resistant proteases [15].

Here, we describe the crystal structure of the G48H mutant of HIV-1 protease in complex with a peptidic inhibitor U-89360E and compare this structure to that of the wild-type HIV-1 protease bound to the same inhibitor [14]. The study of a molecular model of saquinavir resistant mutant protease G48V suggests that the observed structural changes in the G48H HIV-1 protease are generally applicable to other mutants at this position.

2. Experimental procedures

2.1. Enzyme preparation and crystal growth

The recombinant mutant HIV-1 protease G48H was expressed in *E. coli* and purified as previously described [14] with one modification. After refolding, the solution containing the refolded protease was incubated at 37°C for 2 h to complete the proteolysis required to remove extraneous amino acid residues from the protease molecule [16]. This process was monitored by SDS-polyacrylamide gel electrophoresis.

The inhibitor U-89360E was a gift from the Upjohn Co. It is a derivative of Ac-Phe-Val-Gln-Arg-NH_2 in which the peptide bond between Phe and Val has been replaced by a hydroxyethylene moiety (-CHOH-CH_2-) and the phenyl group has been changed to a cyclohexyl group.

The methods employed in the crystallization experiments were essentially the same as described by Hong et al. [14]. The protein solution contained 6.5 mg/ml mutant HIV-1 protease in 20 mM sodium acetate, 1 mM dithiothreitol, pH 5.5, with a 10-fold molar excess of inhibitor. The reservoir solutions for the vapor diffusion contained 10% dimethylsulfoxide, 30 mM β-mercaptoethanol and 4% 2-propanol in addition to the precipitant. The most favorable crystallization conditions were 42% saturated ammonium sulfate, pH 6.8.

2.2. Crystal structure determination

The diffraction data were collected and reduced as described previously [14]. The data collection did not record the entire unique volume of reciprocal space. However, the data recorded was of high quality so that good refinement statistics and clear electron density maps were obtained (see below). The indexing software suggested an orthorhombic space group. Systematic absences of reflections were consistent with an I centered cell, but the choice between space groups I222 and $I2_12_12_1$ could not be made. Since this is a new crystal form for HIV-1 protease, the initial phases were determined by molecular replacement [17], in which a previously determined wild-type HIV-1 protease structure [14] was used as the search model. This calculation was carried out with the molecular replacement program package MRCHK [18]. Diffraction data from resolution 3.6 to 8.0 Å were used for both the rotation and translation searches. The correct rotation function solution was 4.2 σ above the top noise peak. A translation function search in space group I222 confirmed the rotation function search and produced a solution 4.1 σ above the next highest peak. Whereas, in space group $I2_12_12_1$, no translation function solution distinguished itself from the background. Consequently, space group I222 was chosen.

After rigid body and initial positional refinement, the *R*-factor was 0.30 for data from 20.0–2.8 Å. Electron density showed clear inhibitor density with only one inhibitor orientation. Water molecules were added as identified only if their density exceeded 3 σ in the $|F_o|$-$|F_c|$ map and if their position did not produce a violation of van der Waals radii. Statistics for data collection and refinement are summarized in Table 1. Refinements of the crystal structure were carried out using the programs TNT [19] and X-PLOR [20]. Molecular graphics display and calculation of van der Waals surfaces employed the program O using default values for van der Waals calculations

*Corresponding author. Oklahoma Medical Research Foundation, 825 NE 13th St., Oklahoma City, OK 73104. Fax: (1) (405) 271-7249. E-mail: Jordan-Tang@omrf.ouhsc.edu

This work was supported by NIH Grant AI-38189.

PII S0014-5793(97)01477-4

[21]. Since this G48H mutant structure was to be compared to the wild-type HIV-1 protease structure [14], the latter structure was subjected to several cycles of refinement using the TNT and X-PLOR programs so the observed differences would not be due to idiosyncrasies of the refinement procedure.

2.3. Modeling for HIV-1 protease mutant G48V complexed to saquinavir and energetic comparisons

The structural model of HIV-1 protease mutant G48V complexed to saquinavir was built based on the crystal structure of wild-type HIV-1 protease complexed to saquinavir [22] obtained from HIV Protease Structure Data Base [23]. A best fit side-chain conformation of Val^{48} was selected from the most preferred rotomer library. This model of the G48V enzyme-saquinavir complex was subjected to energy minimization calculations using X-PLOR's conjugate gradient energy minimization algorithm. Topology and parameter dictionaries were built for the inhibitor using the bond lengths and angles from the crystal structure as the ideal values. Harmonic coordinate restraints were applied to the C_α atoms of the enzyme during the minimization. For both the wild-type and the mutant structures, the binding energies between saquinavir and each subsite of the protease were calculated using X-PLOR's energy functions. To avoid bias generated by the calculations, the models of the wild-type and mutant enzyme complexes were subjected to the same energy minimization regimens prior to the binding energy comparison.

3. Results and discussion

3.1. Structure of HIV-1 protease mutant G48H and comparison to the wild-type enzyme

The structural comparison of G48H and the wild-type HIV-1 protease (Fig. 1) revealed the most dramatic difference at the side chain of Phe^{B53}. In the structure of the wild-type HIV-1 protease bound to the same inhibitor [14], no van der Waals contact is present between the side chain of Phe^{B53} and the rest of the enzyme dimer. In the structure of the G48H mutant protease, the side chain of Phe^{B53} is at a different position and has considerable van der Waals interaction with the mutated side chain of His^{B48} (Fig. 2). Although the positions of Phe^{A53} side chains in the two structures are similar, in the mutant structure Phe^{A53} side chain is again in van der Waals contacts with His^{A48} as in the B monomer. Additionally, His^{B48} favorably interacts with the bound inhibitor at the backbone atoms in the P_2' and P_3' subsites and with the β, γ, and δ carbon atoms of the Arg side chain of inhibitor subsite P_3'. These interactions are shown in Fig. 2.

Changes in the positions of main chain atoms were observed at surface locations (Fig. 1). Most changes were at β-turns but there also was movement at residue 44 in both monomers (Fig. 1). Although changes of backbone torsion angles at residues 44 and 45 have been suggested as associated with flap opening [24], the currently observed shift does not cause relocation of the flaps.

3.2. Functional consequences of G48H mutation

The side chains of the flap residues in the mutant G48H enzyme are less mobile than the corresponding flap residues in the wild-type protease. This is indicated from a comparison of the crystallographic temperature factors of the main chain atoms in two structures (Fig. 3). In the wild-type complex, the B-monomer flap has less mobility than in the A monomer as the result of interaction with the inhibitor. Consequently the change induced by mutation is not so great in B-monomer (Fig. 3). This increased rigidity in the G48H mutant is most likely a direct consequence of the interactions between Phe^{53} and His^{48} discussed above. The new His^{48} side chain also creates a second effect. In the crystal structure, His^{B48} side chain interacts with the P_2' and P_3' residues of the inhibitor which is expected to stabilize the complexes between the mutant enzyme to the inhibitor and possibly substrates.

Since the crystal forms are different in the G48H mutant and the wild-type enzyme structures, it needs to be established that the change in thermal parameters is not a consequence of altered crystal packing. In fact for both flap regions (A45–A55 and B47–B53) where diminished mobility is seen for the mutant, there are more intermolecular contacts in the wild-type crystal than in the mutant one. Therefore, the stabilization of the flap in the mutant structure occurs even though there is less constriction by intermolecular contacts than in the wild-type structure. Additional deviant regions in Fig. 3, viz. A18–A22, A41–A44, A69–A72, and B18–B22, have thermal parameter change as predicted by the number of crystal contacts. The region A57–A60 which is more rigid in the mutant structure has no intermolecular contacts in either the mutant or the wild-type enzyme crystal structures.

The observation that flap mutation produced structural rigidity contrasts strongly with the observations from previous crystallographic studies of resistant mutants of HIV-1 protease, including V82A [11], V82D, V82N [14], A71T/V82A [12] and a quadruple mutant M46I/L63P/V82T/I84V [13]. In all these cases, the residue replacements are associated with substrate side-chain binding sites; these mutations led to

Table 1
Crystallographic statistics of the wild type and G48H mutant HIV-1 proteases in complex with inhibitor U-89360E

	G48H	Wild type[a]
Space group	I222	$P6_1$
Unit cell (Å)	$a = 58.5$, $b = 88.2$, $c = 94.2$	$a = b = 63.2$, $c = 83.6$
Observed reflections	25 380	27 072
Unique reflections	8697	7669
R_{sym}[b]	0.073	0.039
Data completeness (%) (20.0–2.3 Å)	77.9	90.7
Data completeness (%) (2.42–2.30 Å)	52.6	71.7
R-factor[c]	0.185	0.168
Bond length rms deviation from ideal (Å)	0.013	0.013
Bond angle rms deviation from ideal (deg)	1.8	1.8
Number of water molecules	59	78
B-factor (Å^2) average for protein atoms	36.6	28.1

[a]Data from Hong et al. [14] are included for comparison.
[b]$R_{sym} = \sum\sum |I_{i(h)} - \langle I_{(h)}\rangle| / \sum I_{i(h)}$.
[c]*R*-factor $= \sum ||F_o| - |F_c|| / \sum |F_o|$, where F_o and F_c are the observed and calculated structure factors. The *R*-factors are reported for the range 8.0 to 2.3 Å.

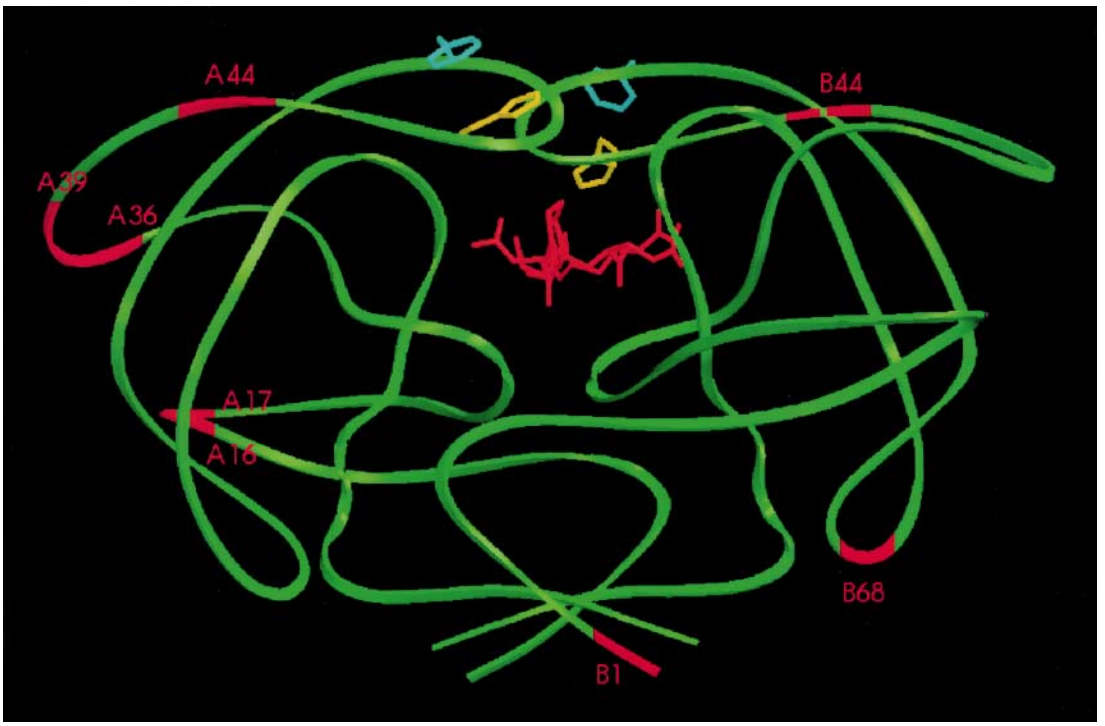

Fig. 1. Backbone ribbon drawing of G48H HIV-1 protease in complex with the inhibitor U-89360E. Side chains for His^{48} (yellow) and Phe^{53} (blue) are shown. The inhibitor molecule (red) within the binding cleft is also depicted. Backbone regions which have significant positional deviations between the mutant and wild-type enzymes are high-lighted in red.

structural changes including gaps or overlaps between van der Waals spaces of inhibitor and enzyme [11–14] and conformational adjustments of the mutant enzyme [11,12]. Since the flaps of the wild-type HIV-1 protease have an unusually high mobility, the rigidity resulting from the mutation at Gly^{48} and possibly other flap residues is likely a common phenomenon.

3.3. Structural model of HIV-1 protease mutant G48V-saquinavir complex and functional implications

The interactions and stabilizing effects described above for the G48H mutant enzyme are likely present in other Gly^{48} mutants of HIV-1 protease. A well documented in vivo resistant mutation of HIV-1 protease against saquinavir therapy is mutant G48V [4]. To further assess the functional effect of mutation at position 48, a model structure for G48V HIV-1 protease bound to saquinavir was constructed based on the structure of the wild-type HIV-1 protease in complex with saquinavir [22]. In this model, the favorable van der Waals contacts between Phe^{53} and Val^{48} and between Val^{48} and saquinavir are clearly present (Fig. 4). These contacts persisted in the model throughout the energy minimization cycles. These new interactions (Fig. 4), which do not occur in the wild-type HIV-1 protease complexed to saquinavir, should

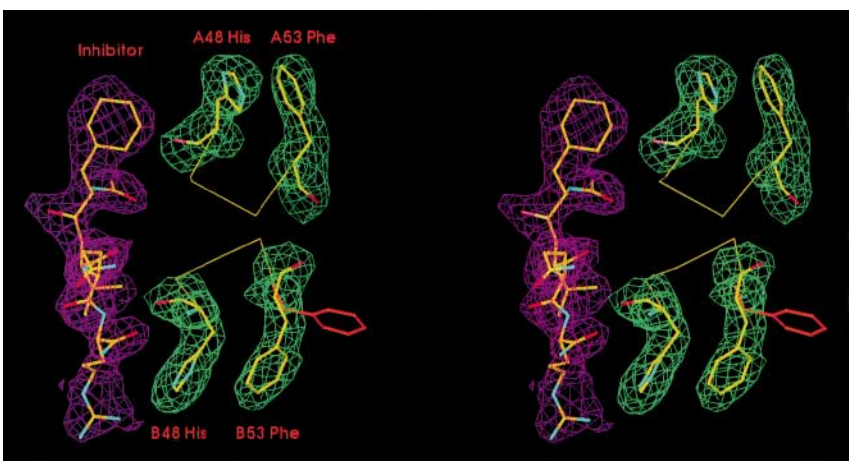

Fig. 2. Stereo view of the structural relationship of the inhibitor molecule and protease residues 48A, 53A, 48B and 53B. Electron densities from the $2|F_o|-|F_c|$ map are shown at 1 σ contour level. A C_α to C_α backbone trace for residues 48 to 53 is included. The position of the side chain of residue B53 in the wild-type structure is also shown (orange).

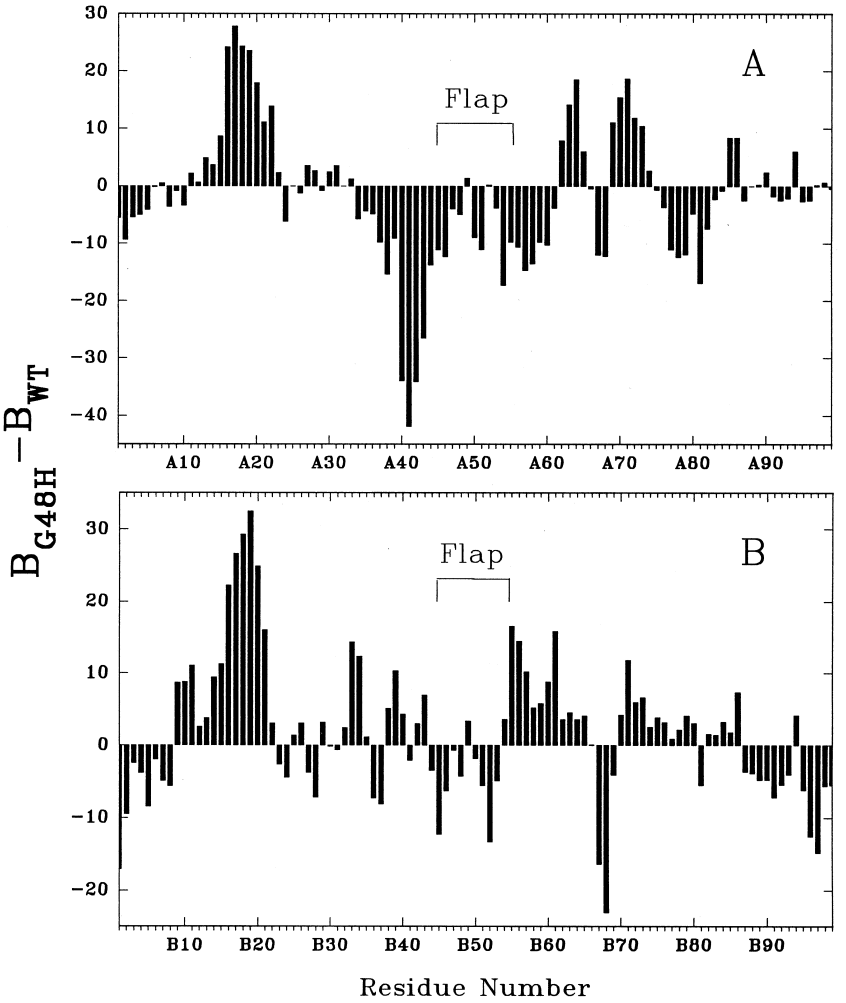

Fig. 3. Average main-chain thermal parameter difference between G48H and wild-type protease. After normalization of wild-type thermal parameters to those of the G48H mutant, the mean crystallographic thermal parameter for each residue in the wild-type enzyme complex is subtracted from that of the G48H mutant. Panels A and B are for the A and B monomers of the HIV-1 protease, respectively. The residues within the flap (45–55) are identified and fall well below the zero line.

have a significant effect on the properties of the mutant enzyme.

It has been argued that the resistant mutation of HIV-1 protease can arise from either the decrease of inhibitor sensitivity or the increase of catalytic efficiency of the mutant enzyme [25]. Several flap mutants of HIV-1 protease are known to retain a significant portion of the catalytic capability of the wild-type enzyme [8,13,26]. For example, the k_{cat} values for the hydrolysis of a peptide (Val-Ser-Gln-Asn-Tyr/Por-Ile-Val-Gln) derived from the cleavage site between HIV-1 matrix and capsid proteins are very close for the wild-type HIV-1 protease (51.8 s^{-1}) and for G48V mutant protease (31.4 s^{-1}) [10]. For some substrates, the k_{cat}/K_m is even greater for several Gly^{48} mutants, including G48H (Lin et al., 1995) and G48V mutant proteases [10], than for the wild-type enzyme. The similarity between the interactions of G48H enzyme (Fig. 2) and the G48V enzyme (Fig. 4) suggests that the decrease of flap mobility and the additional favorable interactions between the mutant enzyme and the substrates most likely contribute to the preserving of catalytic activity.

A relatively small 13.5-fold increase of K_i for the G48V mutant HIV-1 protease compared to that of the wild-type enzyme contributes favorably to the saquinavir resistance [10]. Current structural models provide an opportunity to critically evaluate the interactions of inhibitors with the Gly^{48} mutant enzymes and with the wild-type HIV-1 protease. In order to better define and quantify binding interactions in the crystal structures and models, the van der Waals binding energies and total binding energies were calculated from the structures for the following enzyme-inhibitor pairs: G48H mutant enzyme bound to inhibitor U-89360E, G48V mutant enzyme bound to saquinavir, and the wild-type HIV-1 protease bound separately to each of these two inhibitors. For the G48H mutant complex, van der Waals binding interactions to inhibitor U-89360E are more favorable than those in the wild-type enzyme bound to the same inhibitor (Fig. 5A). The differences are primarily attributable to the new interactions discussed above between the inhibitor and residues of the protease flap. This additional stabilization of mutant enzyme-inhibitor complex by van der Waals interactions does not carry through to the free energy of binding, since the K_is for the U-89360E are 119 nM for G48H and 20 nM for the wild-type protease [8]. The X-PLOR calculations indicate that the destabilizing factor in the G48H protease-inhibitor complex is relatively unfavorable electrostatic interactions for the Arg side chain of the U-89360E inhibitor to the mutant en-

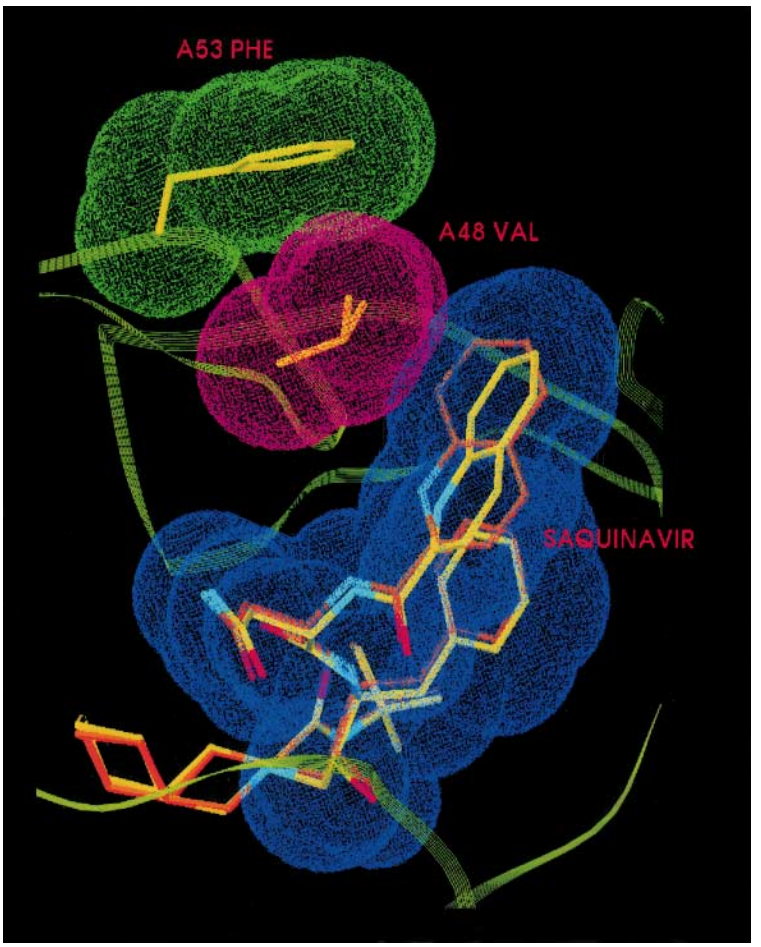

Fig. 4. Van der Waals interaction of Phe^{A53}, Val^{A48} and the P_3 subsite of saquinavir in the structural model of HIV-1 mutant protease G48V complex with saquinavir. The saquinavir positions in the wild-type crystal structure (orange) and of the G48V mutant model structure (yellow) are both shown. There is a 30° rotation of the saquinavir P_3 planar quinoline group (double ring) in the G48V complex compared to that in the wild-type enzyme. This change appears to be a result of its interaction with Val^{48}. The van der Waals interaction between Val^{48} and Phe^{53} is shown but the view does not minimize overlap of the surfaces.

zyme. The aggregate van der Waals interaction of G48V HIV-1 protease with saquinavir is nearly identical to that in the wild-type protease-saquinavir complex (Fig. 5B). The total binding energy calculated by X-PLOR is less favorable for the G48V complex with saquinavir than for the wild-type protease complex (Fig. 5B). The predominant difference between these complexes is an electrostatic destabilization in the mutant complex especially in the P_1 subsite of saquinavir. The

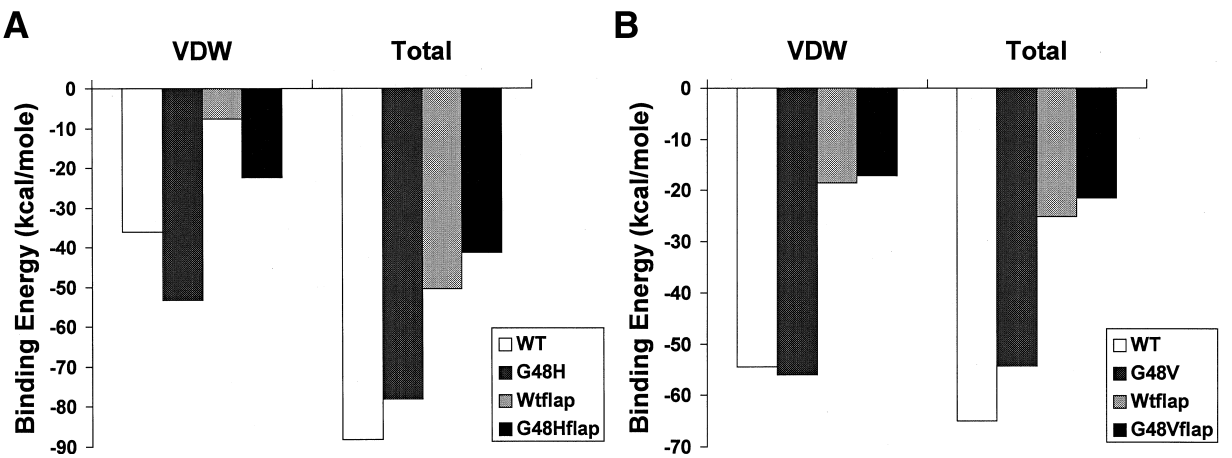

Fig. 5. Comparison of van der Waals and total binding energies. Van der Waals (VDW) and total binding energy (Total) are shown for the interaction of the inhibitor with the wild-type HIV-1 protease (WT), the mutant protease, the flap residues (45–55) of the WT and mutant protease. A: Energy is evaluated for the refined crystal structures of G48H and wild-type HIV-1 protease bound to U-89360E. B: Energy is evaluated for the models of G48V and wild-type HIV-1 protease bound to saquinavir after energy minimization.

greater binding energy calculated for the wild-type complex than for the G48V mutant is consistent with the free energy of binding. The K_is for saquinavir inhibition of wild-type HIV-1 protease and the G48V mutant are 0.2 and 2.7 nM, respectively [10]. These energetic comparisons illustrate an interesting point. Even though the new G48 side chains interact similarly with other enzyme groups and inhibitors as shown in Fig. 2 Fig. 5, these interactions have different impact on the total van der Waals binding energy of inhibitors.

From the crystal structure, the model building experiment and the energetic calculations, one is able to conclude that the interaction between Phe^{53} and a mutant side chain at residue 48 is probably a general structural feature of Gly^{48} mutants of HIV-1 protease. Total binding energy is not a direct consequence of the productive van der Waals interactions visible in crystal structures. For U-89360E, van der Waals interactions with the G48H mutant are more favorable than for the wild-type protease. There seems to be no net change in the van der Waals energy for saquinavir binding to the G48V mutant compared to the wild-type protease. For both comparisons made herein, the total binding energy is less for inhibitor binding to the mutant protease than to the wild-type protease (Fig. 5).

The structural observations detailed above may be applicable to other mutations in the HIV-1 protease flap. In the molecular dynamics modeling studies of Collins et al. [24], the M46I mutant demonstrated noticeably less flap flexibility than the wild-type HIV-1 protease. Moreover, the simian immunodeficiency virus protease is homologous to HIV-1 protease except that residue 46 is isoleucine. In the structure of that protease in complex with an inhibitor, Phe^{53} makes van der Waals contact with Ile^{46} [27]. This provides yet another example of stabilizing interactions between Phe^{53} and side chains at either position 46 or 48 in these mutant proteases. We suggest that this is a usual case for mutations in the flap region of HIV-1 protease.

Acknowledgements: The authors thank Mr. Marcus Dehdarani for excellent technical assistance, Dr. Vladamir Nauchitel for several fruitful discussions, and Drs. W.L. Thaisrivongs and R.L. Heinrikson for the gift of inhibitor U-89360E.

References

[1] Coffin, J.M. (1995) Science 267, 483–489.
[2] Condra, J.H., Schleif, W.A., Blahy, O.M., Gabryelski, L.J., Graham, D.J., Quintero, J.C., Rhodes, A., Robbins, H.L., Roth, E., Shivaprakash, M., Titus, D., Yang, T., Teppler, H., Squires, K.E., Deutsch, P.J. and Emini, E.A. (1995) Nature 374, 569–571.
[3] Molla, A., Korneyeva, M., Gao, Q., Vasavanonda, S., Schipper, P.J., Mo, H.M., Markowitz, M., Chernyavskiy, T., Niu, P., Lyons, N., Hsu, A., Granneman, G.R., Ho, D.D., Boucher, C.A., Leonard, J.M., Norbeck, D.W. and Kempf, D.J. (1996) Nat. Med. 2, 760–766.
[4] Jacobsen, H., Hnggi, M., Ott, M., Duncan, I.B., Owen, S., Andreoni, M., Vella, S. and Mous, J. (1996) J. Infect. Dis. 176, 1379–1387.
[5] Craig, J.C., Duncan, I.B., Hockley, C., Grief, N.A., Roberts, N.A. and Mills, J.S. (1991) Antiviral Res. 16, 295–305.
[6] Dorsey, B.D. and Huff, J.R. et al. (1994) J. Med. Chem. 37, 3443–3451.
[7] Kempf, D.J. and Norbeck, D.W. et al. (1995) Proc. Natl. Acad. Sci. USA 92, 2484–2488.
[8] Lin, Y., Lin, X., Hong, L., Foundling, S., Heinrikson, R.L., Thaisrivongs, S., Leelamanit, W., Raterman, D., Shah, M., Dunn, B.M. and Tang, J. (1995) Biochemistry 34, 1143–1152.
[9] Maschera, B., Darby, G., Palu, G., Wright, L.L., Tisdale, M., Myers, R., Blair, E.D. and Furfine, E.S. (1996) J. Biol. Chem. 271, 33231–33235.
[10] Ermolieff, J., Lin, X. and Tang, J. (1997) Biochemistry 36, 12364–12370.
[11] Baldwin, E.T., Bhat, T.N., Liu, B., Pattabiraman, N. and Erickson, J. (1995) Nature Struct. Biol. 2, 244–249.
[12] Kervinen, J., Thanki, N., Zdanov, A., Tino, J., Barrish, J., Lin, P.F., Colonno, R., Riccardi, K., Samanta, H. and Wlodawer, A. (1996) Protein Pept. Lett. 3, 399–406.
[13] Chen, Z., Li, Y., Schck, H.B., Hall, D., Chen, E. and Kuo, L.C. (1995) J. Biol. Chem. 270, 21433–21436.
[14] Hong, L., Treharne, A., Hartsuck, J.A., Foundling, S. and Tang, J. (1996) Biochemistry 35, 10627–10633.
[15] Mellors, J.W., Larder, B.A. and Schinazi, R.F. (1994) Int. Antiviral News 3, 8–13.
[16] Ido, E., Han, H.P., Kezdy, F.J. and Tang, J. (1991) J. Biol. Chem. 266, 24359–24366.
[17] Rossman, M.G., Ed. (1972) The Molecular Replacement Method, Gordon and Breach, New York.
[18] Zhang, X.-J. and Matthews, B.W. (1994) Acta Cryst. D50, 675–686.
[19] Tronrud, D.E., Ten Eyck, L.F. and Matthews, B.W. (1987) Acta Cryst. A43, 489–503.
[20] Brunger, A.T. (1992) X-PLOR Version 3.1: A System for X-ray Crystallography and NMR, Yale University Press, New Haven.
[21] Jones, T.A., Zou, J.-Y., Cowna, S.W. and Kjeldgaard, M. (1991) Acta Cryst. A47, 110–119.
[22] Krohn, A., Redshaw, S., Ritchie, J.C., Graves, B.J. and Hatada, M.H. (1991) J. Med. Chem. 34, 3340–3342.
[23] Vondrasek, J., van Buskirk, C.P. and Wlodawer, A. (1997) Nature Struct. Biol. 4, 8.
[24] Collins, J.R., Burt, S.K. and Erickson, J.W. (1995) Nature Struct. Biol. 2, 334–338.
[25] Tang, J. and Hartsuck, J.A. (1995) FEBS Lett. 367, 112–116.
[26] Shao, W., Everitt, L., Manchester, M., Loeb, D.D., Hutchison, C.A. and Swanstrom, R. (1997) Proc. Natl. Acad. Sci. USA 94, 2243–2248.
[27] Zhao, B., Winborne, E., Minnich, M.D., Culp, J.S., Debouck, C. and Abdel-Meguid, S.S. (1993) Biochemistry 32, 13054–13060.